ISSN 0005-1179 (print), ISSN 1608-3032 (online), Automation and Remote Control, 2023, Vol. 84, No. 1, pp. 82–95.

Iterative Learning Control of a Discrete-Time System under Delay along the Sample Trajectory and Input Saturation

P. V. Pakshin[*,a] **and J. P. Emelyanova**[*,b]

[*]*Arzamas Polytechnic Institute of R.E. Alekseev Nizhny Novgorod State Technical University, Arzamas, Russia*
e-mail: [a]*pakshinpv@gmail.com*, [b]*emelianovajulia@gmail.com*

Received August 19, 2022
Revised September 19, 2022
Accepted September 29, 2022

Abstract—This paper considers a linear discrete-time system operating in a repetitive mode to track a reference trajectory with a required accuracy. The control variable has a delay along the sample trajectory, and saturation-type constraints are imposed. We introduce a new method for designing an iterative learning control law that depends on the delay and ensures the required accuracy of tracking. A numerical example demonstrates the effectiveness of this method.

Keywords: iterative learning control, input saturation, delay, repetitive processes, 2D systems, stability, stabilization, vector Lyapunov function, linear matrix inequalities

DOI: 10.25728/arcRAS.2023.72.77.001

1. INTRODUCTION

Iterative learning control (ILC) is an effective tool to improve accuracy in systems operating in a repetitive mode [1]. A simple typical example of such systems is a gantry robot placing components in desired positions on a conveyor. Currently, iterative learning control algorithms find application in robotic-assisted upper-limb stroke rehabilitation [2, 3], in ventricular assist devices [4], laser metal deposition [5, 6], and other repetitive processes [6–8].

Most ILC design works involve linear models [9, 10]. At the same time, actuators of robotic systems are often electromechanical devices with characteristic nonlinearities (saturation, dead zone, backlash, and hysteresis). These nonlinearities can make the required accuracy unachievable and therefore need a detailed study. Delays, particularly those arising under remote control, are another factor neglected within linear models.

These factors in ILC problems were analyzed by several researchers. Nevertheless, no exhaustive solution has been provided so far. In this paper, we consider input saturation as a widespread nonlinearity. Different ILC algorithms for systems with saturation constraints were proposed in [11–17]. However, none of the authors cited above discussed the effect of saturation level on accuracy. As demonstrated therein, the algorithms reduce the learning error, but its steady-state value (as the number of passes increases) was not investigated depending on the saturation level.

ILC reflects an important feature of repetitive processes: the learning error signals from previous passes contain essential information, and all ILC algorithms efficiently use this information on the current pass. ILC differs from other control strategies with learning, such as adaptive control and neural network control. Adaptive control changes controller parameters, whereas ILC changes only the input signal. In addition, adaptive controllers typically do not use the information contained in repetitive command signals. Similarly, training a neural network involves changing controller parameters by modifying this network. Neural networks often need large amounts of training data, and it may be difficult to ensure fast convergence. In contrast, ILC algorithms usually converge adequately in only a few iterations; see [9] and references in [9].

Due to the described feature of ILC laws, different cases are possible: delays in the state and control vectors on each pass or delays along the passes. (In the latter case, the information available on the current pass corresponds not to the previous pass but to an earlier one.) Different ILC algorithms for systems with state delays were proposed in [18–23]. As far as we know, other types of delays have not been considered in the literature.

This paper develops the results of [24] for systems with input saturation and delay along the sample trajectory. Both factors have not been simultaneously analyzed in the literature. (Although, their combination is quite natural in engineering; see an illustrative example below.) As in [24], we construct a 2D model in the repetitive process form [25] and employ the divergent method of vector Lyapunov functions [26]. Due to this approach, the final results are obtained using an efficient technique of linear matrix inequalities (LMIs). Note that the proposed ILC algorithm depends on the delay. An illustrative example is given, and some lines of further research are indicated.

2. PROBLEM STATEMENT

Consider a linear discrete-time system operating in a repetitive mode. On pass (iteration or trial) k, the system dynamics are described by the state-space model

$$\begin{aligned} x_k(p+1) &= Ax_k(p) + B\psi_k(p-d), \\ \psi_k(p) &= \mathrm{sat}(u_k(p)), \\ y_k(p) &= Cx_k(p),\ p \in [0, N-1],\ k = 0, 1, \ldots, \end{aligned} \tag{2.1}$$

where: $x_k(p) \in \mathbb{R}^{n_x}$, $u_k(p) \in \mathbb{R}^{n_u}$, and $y_k(p) \in \mathbb{R}^{n_y}$ denote the state vector, control vector, and pass profile, respectively; N is the pass duration; d is the number of delay steps; $\psi_k(p) \in \mathbb{R}^{n_u}$ is the saturation function given by

$$\psi_k(p)_j = \mathrm{sat}(u_k(p))_j = \begin{cases} U_j \ \text{ if } \ u_{k,j}(p) > U_j, \\ u_{k,j}(p) \ \text{ if } \ -U_j \leqslant u_{k,j}(p) \leqslant U_j, \\ -U_j \ \text{ if } \ u_{k,j}(p) < -U_j, \end{cases} \tag{2.2}$$

for $1 \leqslant j \leqslant n_u$ and $k \geqslant 0$, where $u_{k,j}(p)$ denotes the jth component of $u_k(p)$ and U_j is a positive constant.

Let $y_{ref}(p)$, $0 \leqslant p \leqslant N$, be a given reference trajectory (desired pass profile). Then

$$e_k(p) = y_{ref}(p) - y_k(p) \tag{2.3}$$

is the learning error on pass k.

The ILC design problem is to construct a sequence of control inputs $u_k(p)$, bounded for all $k = 0, 1, \ldots,$ to track the reference trajectory in a finite number k^* of passes with a given accuracy:

$$||e_k(p)|| \leqslant e^*,\ k \geqslant k^*,\ 0 \leqslant p \leqslant N. \tag{2.4}$$

3. TRANSITION TO AN EQUIVALENT 2D MODEL IN THE REPETITIVE PROCESS FORM

This problem will be solved if the sequence $u_k(p)$ satisfies the following convergence conditions:

$$\begin{aligned}&\lim_{k\to\infty}||e_k(p)|| = ||e_\infty(p)||,\\&||e_k(p)|| \leqslant \kappa\varrho^k + \mu,\ \ \kappa > 0,\ \ \mu \geqslant 0,\ \ 0 < \varrho < 1,\\&\lim_{k\to\infty}||u_k(p)|| = ||u_\infty(p)||,\end{aligned} \tag{3.1}$$

where $u_\infty(p)$ is a bounded variable usually called the learned control.

We design the ILC law on the current pass in the form

$$\psi_{k+1}(p) = \mathrm{sat}(u_{k+1}(p)),\ \ u_{k+1}(p) = \mathrm{sat}(\psi_k(p) + \delta u_{k+1}(p)), \tag{3.2}$$

where $\delta u_{k+1}(p)$ is the control update for ensuring the convergence conditions (3.1).

Following the standard procedure, let us pass from (2.1) to an equivalent extended model. For this purpose, we introduce an auxiliary vector $\hat{x}_k$ of dimension dn_u with the components $\hat{x}_{ki}(p) = \psi_k(p - i)$, $i = 1, \ldots, d$. Obviously, this vector satisfies the equation

$$\hat{x}_k(p + 1) = A_d\hat{x}_k(p) + B_d\psi_k(p), \tag{3.3}$$

where

$$A_d = \begin{bmatrix} 0 & 0 & \ldots & 0 & 0\\ I & 0 & \ldots & 0 & 0\\ 0 & I & \ldots & 0 & 0\\ \vdots & \vdots & \ddots & \vdots & \vdots\\ 0 & 0 & \ldots & I & 0\end{bmatrix},\ \ B_d = [I\ 0\ 0 \ldots 0]^T.$$

Therefore, the first equation in (2.1) can be written as

$$x_k(p + 1) = Ax_k(p) + BC_d\hat{x}_k(p), \tag{3.4}$$

where $C_d = [\underbrace{0 \ldots 0}_{d-1}\ I]$.

Denoting $\bar{x}_{k+1}(p) = [x^T_{k+1}(p)\ \hat{x}^T_{k+1}(p)]^T$, we represent (3.3), (3.4) as the single equation

$$\begin{aligned}\bar{x}_k(p + 1) &= \hat{A}\bar{x}_k(p) + \hat{B}\psi_k(p),\\ y_k(p) &= \hat{C}\bar{x}_k(p),\end{aligned} \tag{3.5}$$

where

$$\hat{A} = \begin{bmatrix} A & BC_d\\ 0 & A_d\end{bmatrix},\ \ \hat{B} = \begin{bmatrix} 0\\ B_d\end{bmatrix},\ \ \hat{C} = [C\ 0].$$

Assume that the state vector is available for control design and the matrix CB is nonsingular. In the case of no delay, the nonsingularity condition allows deriving a simple equation for the learning error as a function of the number of passes. For the extended model, $\hat{C}\hat{B} = 0$, and additional transformations are needed. First, we obtain equations for the increments of the extended state vector. Let us introduce the auxiliary variable

$$\eta_{k+1}(p + 1) = \bar{x}_{k+1}(p) - \bar{x}_k(p). \tag{3.6}$$

According to (3.5), this variable satisfies the equation

$$\eta_{k+1}(p+1) = \hat{A}\eta_{k+1}(p) + \hat{B}\Delta\psi_{k+1}(p-1), \tag{3.7}$$

where $\Delta\psi_{k+1}(p-1) = \psi_{k+1}(p-1) - \psi_k(p-1)$. Due to the structure of the matrices $\hat{A}$ and $\hat{B}$,

$$\hat{C}\hat{A}^d\hat{B} = CB. \tag{3.8}$$

Consider the biased learning error $\bar{e_k}(p) = e_k(p+d)$. In view of (2.3), (3.5)–(3.7), it is described by the equation

$$\bar{e}_{k+1}(p) = -\hat{C}\hat{A}^{d+1}\eta_{k+1}(p) + \bar{e}_k(p) - CB\Delta\psi_{k+1}(p-1). \tag{3.9}$$

Note that, like the state variables, the variable $\hat{x}_{kd}$ is also available for ILC design in (3.2). Therefore, we have additional information for ILC design and determine the control update as

$$\delta u_{k+1}(p) = K_1\eta_{k+1}(p+1) + K_2\bar{e}_k(p+1), \tag{3.10}$$

where the matrix K_1 is given by

$$K_1 = [\underbrace{K_{11}}_{n_x}\ \underbrace{0\ldots 0}_{(d-1)n_u}\ \underbrace{K_{12}}_{n_u}].$$

Substituting (3.10) into (3.7) and (3.9) yields

$$\begin{aligned} \eta_{k+1}(p+1) &= (\hat{A} + \hat{B}K_1)\eta_{k+1}(p) + \hat{B}K_2\bar{e}_k(p) + \hat{B}\varphi_k(p), \\ \bar{e}_{k+1}(p) &= -(\hat{C}\hat{A}^{d+1} + CBK_1)\eta_{k+1}(p) \\ &\quad + (I - CBK_2)\bar{e}_k(p) - CB\varphi_k(p), \end{aligned} \tag{3.11}$$

where $\varphi_k(p) = \Delta\psi_{k+1}(p-1) - \delta u_{k+1}(p-1)$. Let us denote

$$K = \begin{bmatrix} K_1 & K_2 \end{bmatrix},\ \zeta_k(p) = \begin{bmatrix} \eta^T_{k+1}(p) & \bar{e}^T_k(p) \end{bmatrix}^T.$$

Due to (2.2),

$$-2U_j \leqslant \text{sat}(u_{k+1}(p))_j - \text{sat}(u_k(p))_j \leqslant 2U_j,\ j = 1, \ldots, n_u. \tag{3.12}$$

According to (2.2) and (3.10), the components of the function $\varphi_k(p)$ obviously satisfy the constraints

$$\begin{aligned} F_j[(\varphi_k(p))_j, (\zeta_k(p))_j] = &\left[1 + \frac{1}{2U_j}((\varphi_k(p))_j + (K\zeta_k(p))_j)\right] \\ &\times \left[1 - \frac{1}{2U_j}((\varphi_k(p))_j + (K\zeta_k(p))_j)\right] \geqslant 0,\ j = 1, 2, \ldots, n_u. \end{aligned} \tag{3.13}$$

System (3.11) belongs to the class of nonlinear repetitive processes representing the most widespread particular case of $2D$ systems [25].

4. ILC DESIGN BASED ON THE DIVERGENT METHOD OF VECTOR LYAPUNOV FUNCTIONS

Consider the following vector Lyapunov function on the trajectories of system (3.11):

$$V(\eta_{k+1}(p), \bar{e}_k(p)) = \begin{bmatrix} V_1(\eta_{k+1}(p)) \\ V_2(\bar{e}_k(p)) \end{bmatrix}, \tag{4.1}$$

where $V_1(\eta_{k+1}(p)) > 0$, $\eta \neq 0$, $V_2(\bar{e}_k(p)) > 0$, $\bar{e}_k(p) \neq 0$, $V_1(0) = 0$, and $V_2(0) = 0$. We define the discrete analog of the divergence operator along the trajectories of this system as

$$\mathcal{D}_d V(\eta_{k+1}(p), \bar{e}_k(p)) = V_1(\eta_{k+1}(p+1)) - V_1(\eta_{k+1}(p)) + V_2(\bar{e}_{k+1}(p)) - V_2(\bar{e}_k(p)). \tag{4.2}$$

Theorem 1. *If there exist a vector Lyapunov function* (4.1), *positive numbers* c_1, c_2, *and* c_3, *and a nonnegative number* γ *such that*

$$c_1||\eta_k(p)||^2 \leqslant V_1(\eta_k(p)) \leqslant c_2||\eta_k(p)||^2, \tag{4.3}$$

$$c_1||\bar{e}_k(p)||^2 \leqslant V_2(\bar{e}_k(p)) \leqslant c_2||\bar{e}_k(p)||^2, \tag{4.4}$$

$$\mathcal{D}_d V(\eta_{k+1}(p), \bar{e}_k(p)) \leqslant \gamma - c_3(||\eta_{k+1}(p)||^2 + ||\bar{e}_k(p)||^2), \tag{4.5}$$

then the convergence conditions (3.1) *hold for system* (3.11).

Proof. In the case $\gamma = 0$, the proof coincides with that of Theorem 1 in [26]. If $\gamma \neq 0$, following the same line of reasoning, we obtain

$$||\bar{e}_k(p-1)||^2 \leqslant \frac{1}{c_1}\left[\lambda^k \sum_{q=0}^{p-1} \lambda^{p-1-q} V_2(\bar{e}_0(q)) + \gamma \sum_{n=0}^{k-1}\left(\sum_{q=0}^{p-1}\lambda^{p-1-q}\right)\lambda^{k-1-n}\right], \tag{4.6}$$

where $0 < \lambda < 1$. Since the value $||\bar{e}_0(q)||^2$ is bounded for all $0 \leqslant q \leqslant N-1$, there exists $\bar{\mu} > 0$ such that $||\bar{e}_0(q)||^2 \leqslant \bar{\mu}$. According to (4.4), we have

$$\sum_{q=0}^{p-1} \lambda^{p-1-q} V_2(\bar{e}_0(q)) \leqslant c_2\bar{\mu} \sum_{q=0}^{\infty} \lambda^{p-1-q} = \frac{c_2\bar{\mu}}{1-\lambda}. \tag{4.7}$$

Considering (4.7), inequality (4.6) implies

$$\begin{aligned} &||\bar{e}_k(p-1)||^2 \leqslant \alpha\lambda^k + \beta, \\ &\alpha = \frac{c_2\bar{\mu}}{c_1(1-\lambda)}, \quad \beta = \frac{\gamma}{c_1(1-\lambda)^2}, \quad 1 \leqslant p \leqslant N. \end{aligned} \tag{4.8}$$

By definition, $\bar{e}_k(p-1)$ is the biased learning error. Hence, condition (4.8) leads to the second inequality of (3.1) with the parameters $\kappa = \sqrt{\alpha}$, $\varrho = \sqrt{\lambda}$, and $\mu = \sqrt{\beta}$. Moreover, by analogy with the derivation of (4.8), we arrive at the upper bound

$$||\eta_k(p)|| \leqslant \kappa\varrho^k + \mu, \ 0 \leqslant p \leqslant N-1. \tag{4.9}$$

Since $\delta u_{k+1}(p)$ is given by (3.10), the upper bounds (4.8) and (4.9) guarantee the existence of $\tilde{\kappa}$ and $\tilde{\mu}$ such that

$$||\delta u_{k+1}(p)|| \leqslant \tilde{\kappa}\varrho^k + \tilde{\mu}$$

for all k and $0 \leqslant p \leqslant N-1$. The second equality of (3.2) yields

$$||u_{k+1}(p)|| \leqslant ||\psi_k(p)|| + ||\delta u_{k+1}(p)||.$$

Due to the boundedness of $\psi_k(p)$ and the latter inequality, the value $||u_k(p)||$ is bounded for all k and $0 \leqslant p \leqslant N-1$, and $||u_\infty(p)|| = \lim\limits_{k\to\infty} ||u_k(p)||$ is bounded as well. Thus, all conditions of (3.1) hold. The proof of Theorem 1 is complete.

Denote

$$\bar{A} = \begin{bmatrix} \hat{A} & 0 \\ -\hat{C}\hat{A}^{d+1} & I \end{bmatrix}, \quad \bar{B} = \begin{bmatrix} \hat{B} \\ -CB \end{bmatrix},$$

$$D_U = \mathrm{diag}[1/4U_j^2], \quad T_U = D_U^{-1}, \quad j = 1, 2 \ldots, n_u, \quad (4.10)$$

and define a matrix $P = \mathrm{diag}[P_1\ P_2] \succ 0$ as the solution of the discrete algebraic Riccati inequality

$$\bar{A}^T P\bar{A} - (1-\sigma)P - \bar{A}^T P\bar{B}[\bar{B}^T P\bar{B} + R]^{-1}\bar{B}^T P\bar{A} + Q \preceq 0, \quad (4.11)$$

where $0 < \sigma < 1$, $Q \succ 0$, and $R \succ 0$. On the right-hand side of the divergence formula, this inequality will serve for separating the relations close to those used in the classical theory of linear-quadratic controller design. In particular, the matrices Q and R are similar in sense to the weight matrices of the classical theory, whereas the parameter σ allows affecting the stability margin. After such transformations, described in detail in the paper [27], it becomes possible to apply the technique of linear matrix inequalities (LMIs). Using the Schur complement lemma, we easily reduce (4.11) to the following LMI in the variable $X = \mathrm{diag}[X_1\ X_2]$ with $X_1 = P_1^{-1}$ and $X_2 = P_2^{-1}$:

$$\begin{bmatrix} (1-\sigma)X & X\bar{A}^T & X \\ \bar{A}X & X + \bar{B}R^{-1}\bar{B}^T & 0 \\ X & 0 & Q^{-1} \end{bmatrix} \succeq 0,\ X \succ 0. \quad (4.12)$$

If this LMI is solvable, then $P = X^{-1}$ and we establish the following result according to the paper [27]: the linear control law without constraints and with the control update (3.10), compactly written as $\delta u_{k+1}(p) = K\zeta_k(p)$, ensures the convergence of the learning error to zero as $k \to \infty$, where

$$K = [K_1\ K_2] = -[\bar{B}^T P\bar{B} + R]^{-1}\bar{B}^T P\bar{A}\Theta, \quad (4.13)$$

Θ is the block diagonal matrix

$$\Theta = \begin{bmatrix} \Theta_1 & 0 \\ 0 & \Theta_2 \end{bmatrix}, \ \Theta_1 = \mathrm{diag}[\underbrace{\Theta_{11}}_{n_x}\ \underbrace{0\ldots0}_{(d-1)n_u}\ \underbrace{\Theta_{12}}_{n_u}],$$

satisfying the LMI

$$\begin{bmatrix} M - M\Theta - \Theta M - Q & \Theta\sqrt{M} \\ \sqrt{M}\Theta & -I \end{bmatrix} \preceq 0 \quad (4.14)$$

with $M = \bar{A}^T P\bar{B}[\bar{B}^T P\bar{B} + R]^{-1}\bar{B}^T P\bar{A}$. The relation (4.14) reflects structural constraints on the matrix K_1 in (3.10). It naturally holds in the absence of such constraints. In the case of no constraints, the control update matrix can be calculated in an alternative way. Let the variables X, Y, and Z be the solution of the system of matrix inequalities and equations

$$\begin{bmatrix} X & (\bar{A}X+\bar{B}YH)^T & X & (YH)^T \\ \bar{A}X+\bar{B}YH & X & 0 & 0 \\ X & 0 & Q^{-1} & 0 \\ YH & 0 & 0 & R^{-1} \end{bmatrix} \succeq 0,$$

$$HX = ZH, \quad X = \mathrm{diag}[X_1\ X_2] \succ 0, \tag{4.15}$$

where

$$H = \begin{bmatrix} I_{n_x} & 0 & \dots & 0 & 0 & 0 \\ 0 & 0 & \dots & 0 & I_{n_u} & 0 \\ 0 & 0 & \dots & 0 & 0 & I_{n_y} \end{bmatrix}.$$

In this case, by the Schur complement lemma, we have the inequality

$$(\bar{A}+\bar{B}\bar{K}H)^T P(\bar{A}+\bar{B}\bar{K}H) - P + Q + (\bar{K}H)^T R\bar{K}H \preceq 0, \tag{4.16}$$

where $P = \mathrm{diag}[P_1\ P_2] = X^{-1} \succ 0$ and

$$\bar{K} = YZ^{-1}. \tag{4.17}$$

Hence, the conditions of Theorem 1 from the paper [26] hold with the quadratic forms

$$\begin{aligned} V_1(\eta_{k+1}(p)) &= \eta_{k+1}^{\mathrm{T}}(p)P_1\eta_{k+1}(p), \\ V_2(\bar{e}_k(p)) &= \bar{e}_k^T(p)P_2\bar{e}_k(p) \end{aligned} \tag{4.18}$$

as the components of the corresponding vector Lyapunov function; moreover, in the system without constraints, the control update $\delta u_{k+1}(p) = \bar{K}H\zeta_k(p)$ ensures the convergence of the learning error to zero as $k \to \infty$.

Theorem 2. *Given the constraints* (3.13) *and some matrices* $Q \succ 0$, $R \succ 0$, *and* Θ, *let there exist a solution* $X = \mathrm{diag}[X_1\ X_2] \succ 0$ *of the combined LMIs* (4.12) *and* (4.14) *such that the LMI*

$$\begin{bmatrix} -W & -(KW)^T & (\bar{A}W+\bar{B}KW)^T \\ -KW & -TT_U & TT_U\bar{B}^T \\ (\bar{A}W+\bar{B}KW) & \bar{B}TT_U & -W \end{bmatrix} \prec 0 \tag{4.19}$$

is solvable in the variables $W = \mathrm{diag}[W_1\ W_2] \succ 0$ *and* $T = \mathrm{diag}[T_j] \succ 0$, $j = 1, \dots, n_u$, *for the matrix* K *given by* (4.13). *Then the ILC law* (3.2), (3.10) *ensures the convergence conditions* (3.1).

Proof. As the components of the vector function (4.1) we choose the quadratic forms (4.18), where $P_1 \succ 0$ and $P_2 \succ 0$, and form the block matrix $P = \mathrm{diag}[P_1\ P_2]$. Since the combined LMIs (4.12) and (4.14) are solvable, let K be given by (4.13). Calculating the divergence (4.2) along the trajectories of (3.11) yields

$$\mathcal{D}_d V(\eta, \bar{e}) = [(\bar{A}+\bar{B}KH)\zeta + \bar{B}_\varphi]^T P[(\bar{A}+\bar{B}KH)\zeta + \bar{B}_\varphi] - \zeta^T P\zeta. \tag{4.20}$$

Due to $V_1(\eta_{k+1}(p)) \succ 0$ and $V_2(\bar{e}_k(p)) \succ 0$, conditions (4.3) and (4.4) of Theorem 1 are valid.

Conditions (4.5) of Theorem 1 will hold under the constraints (3.13) if, for all φ and ζ,

$$\mathcal{D}_d V(\eta, \bar{e}) + \sum_{j=1}^{n_u} d_j F_j[(\varphi_k)_j, (\zeta_k)_j] \leqslant \gamma - \epsilon||\zeta||^2, \tag{4.21}$$

where d_j, $j = 1, \dots, n_u$, are positive constants and ϵ is a sufficiently small positive number [28]. With (4.21) being satisfied for all φ and ζ, we have

$$\mathcal{D}_d V(\eta, \bar{e}) \leqslant \gamma - \epsilon||\zeta||^2$$

for all φ and ζ and, consequently, under the constraints (3.13). Thus, all conditions of Theorem 1 hold, and inequality (4.21) can be written as

$$\mathcal{D}_d V(\eta, e) - \zeta^T (KH)^T DD_U KH\zeta - 2\zeta^T (KH)^T DD_U \varphi \\ - \varphi^T DD_U \varphi + \operatorname{tr}(D) \leqslant \gamma - \epsilon||\zeta||^2, \tag{4.22}$$

where $D = \operatorname{diag}[d_j]$, $j = 1, 2 \dots, n_u$, and ϵ is a sufficiently small positive number.

In the case $n_u = 1$, this approach (the so-called S procedure) ensures that (4.21) is a sufficient and necessary condition for (4.5) under the constraints (3.13); for details, see [29].

For $\gamma = \operatorname{tr}(D)$, condition (4.5) of Theorem 1 holds if

$$[(\bar{A} + \bar{B}KH)\zeta + \bar{B}\varphi]^T P[(\bar{A} + \bar{B}KH)\zeta + \bar{B}\varphi] - \zeta^T P\zeta \\ - 2\zeta^T (KH)^T DD_U \varphi - \varphi^T (t) DD_U \varphi < 0, \tag{4.23}$$

or equivalently,

$$[\zeta^T \ \varphi^T]\bar{M}_i[\zeta^T \ \varphi^T]^T \prec 0,$$

where

$$\bar{M} = \begin{bmatrix} (\bar{A} + \bar{B}KH)^T P(\bar{A} + \bar{B}KH) - P & (\bar{B}^T P(\bar{A} + \bar{B}KH) - DD_U KH)^T \\ \bar{B}^T P(\bar{A} + \bar{B}KH) - DD_U KH & \bar{B}^T P\bar{B} - DD_U \end{bmatrix}.$$

The matrix $\bar{M}$ can be written as

$$\bar{M} = \begin{bmatrix} -P & -(KH)^T DD_U \\ -DD_U KH & -DD_U \end{bmatrix} + \begin{bmatrix} (\bar{A} + \bar{B}KH)^T \\ \bar{B}^T \end{bmatrix} P[(\bar{A} + \bar{B}KH) \ \bar{B}].$$

By the Schur complement lemma, $\bar{M}_i \prec 0$ if and only if

$$\begin{bmatrix} -P & -(KH)^T DD_U & (\bar{A}_i + \bar{B}KH)^T \\ -DD_U(KH) & -DD_U & \bar{B}^T \\ (\bar{A}_i + \bar{B}KH) & \bar{B} & -P^{-1} \end{bmatrix} \prec 0. \tag{4.24}$$

Denoting $W = P^{-1}$ and $T = D^{-1}$ and multiplying (4.24) by $\operatorname{diag}[P^{-1} \ [DD_U]^{-1} \ I]$ on the left and right, we finally arrive at (4.19). The proof of Theorem 2 is complete.

Using the other method for calculating the matrix K, we give an alternative version of this theorem.

Theorem 3. *Given the constraints* (3.13) *and some matrices* $Q \succ 0$ *and* $R \succ 0$, *let there exist a solution* $X = \operatorname{diag}[X_1 \ X_2] \succ 0$, Y, *and* Z *of the combined LMIs* (4.15) *such that the LMI* (4.19) *is solvable in the variables* $W = \operatorname{diag}[W_1 \ W_2] \succ 0$ *and* $T = \operatorname{diag}[T_j] \succ 0$, $j = 1, \dots, n_u$, *for* $K = \bar{K}H$ *with* $\bar{K}$ *given by* (4.17). *Then the ILC law* (3.2), (3.10) *ensures the convergence conditions* (3.1).

5. AN EXAMPLE

Consider the experimental plant model from [30]. It consists of two permanent magnet synchronous motors (PMSMs) with coupled shafts. The first motor (A) is the drive, whereas the second motor (B) generates the load torque. The goal of control is to track a reference trajectory of the drive shaft angle $\theta(t)$. The continuous plant dynamics model has the form

$$T_{\mathrm{e}}(t) = i_{\mathrm{A}}(t)k_{\mathrm{tA}} = J\frac{\mathrm{d}^2\theta(t)}{\mathrm{d}t^2} + b\frac{\mathrm{d}\theta(t)}{\mathrm{d}t} + T_{\mathrm{l}}(t) \tag{5.1}$$

with the following notations: $T_{\mathrm{e}}(t)$ is the electromagnetic torque generated by motor A; k_{tA} is the torque constant of motor A; J is the total mass moment of inertia; b is the resulting friction coefficient; finally, $T_{\mathrm{l}}(t)$ is the load torque generated by motor B. We selected the following values of the parameters: $T_{\mathrm{cA}} = 0.8 \cdot 10^{-3}$ s, $k_{\mathrm{tA}} = 0.93$ N·m/A, $J = 9.3 \cdot 10^{-4}$ kg·m^2, and $b = 2.4 \cdot 10^{-3}$ kg·m^2/s.

The discrete control signal was computed with the sampling time $T_s = 2$ ms and a delay of 1 step. This signal was converted into a control current through zero-order extrapolation and amplification. The resulting discrete-time state-space model has the form

$$\begin{aligned} x_k(p+1) &= Ax_k(p) + Bu_k(p) + Ed_k(p) \\ y_k(p) &= Cx_k(p), \end{aligned} \tag{5.2}$$

where:

$$A = \begin{bmatrix} 1 & 0.0020 & 0.0020 \\ 0 & 0.9949 & 1.9948 \\ 0 & 0 & 0 \end{bmatrix}, \ B = \begin{bmatrix} 0 \\ 0 \\ 1 \end{bmatrix}, \ E = \begin{bmatrix} -0.0021 \\ -2.1450 \\ 0 \end{bmatrix}, \ C = \begin{bmatrix} 1 & 0 & 0 \end{bmatrix},$$

$$x_k(p) = \begin{bmatrix} \theta_k(p) \\ \omega_k(p) \\ i_{\mathrm{A}k}(p) \end{bmatrix}, \ u_k(p) = i_{\mathrm{A}k}^{\mathrm{ref}}(p), \ d_k(p) = T_{\mathrm{l}k}(p);$$

on pass k, $\theta_k(p)$ is the drive shaft angle, $\omega_k(p)$ is the angular velocity of the drive shaft, $i_{\mathrm{A}k}(p)$ is the current on motor A, $i_{\mathrm{A}k}^{\mathrm{ref}}(p)$ is the control current, and $T_{\mathrm{l}k}(p)$ is the load torque.

According to the previous section, the ILC law has the form

$$u_k(p) = \mathrm{sat}\big(u_{k-1}(p) + K_1(x_k(p) - x_{k-1}(p)) + K_2 e_{k-1}(p+2)\big). \tag{5.3}$$

where K_1 and K_2 are calculated using Theorem 2. When solving the LMIs (4.12), (4.14), we selected the parameters

$$\begin{aligned} &Q = \mathrm{diag}[0.2 \cdot 10^6 \ 10^4 \ 10^4 \ 10^{10}], \ R = 1.5, \ \sigma = 0.9, \\ &\Theta = \mathrm{diag}[1 \ 1 \ 1 \ 1.2]. \end{aligned}$$

With these parameters, inequality (4.19) holds for all saturation levels considered below. As a result, we obtained

$$K_1 = [-30.1869 \ \ -0.5717 \ \ -1.0856], \quad K_2 = 14.3028.$$

In the case of no control constraints, the maximum value of the control signal was 4.7 A. We assessed the effect of the constraint level on the tracking accuracy by the root-mean-square (RMS)

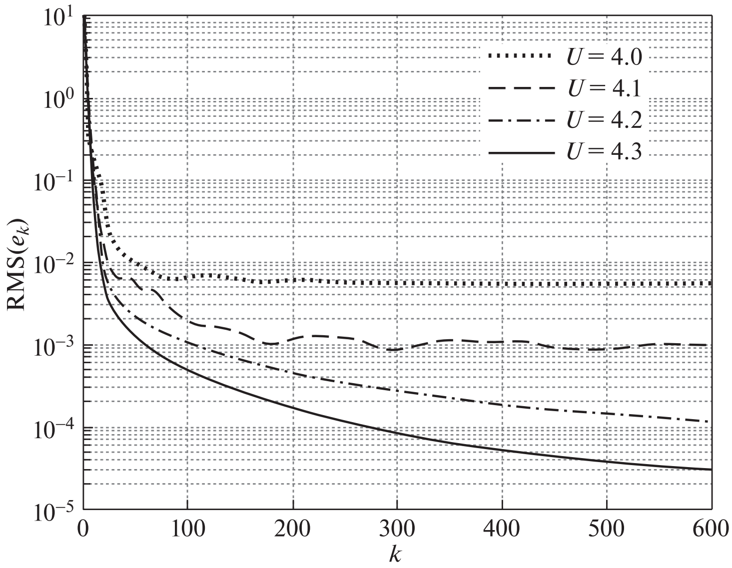

Fig. 1. RMS values of the learning error under different saturation levels.

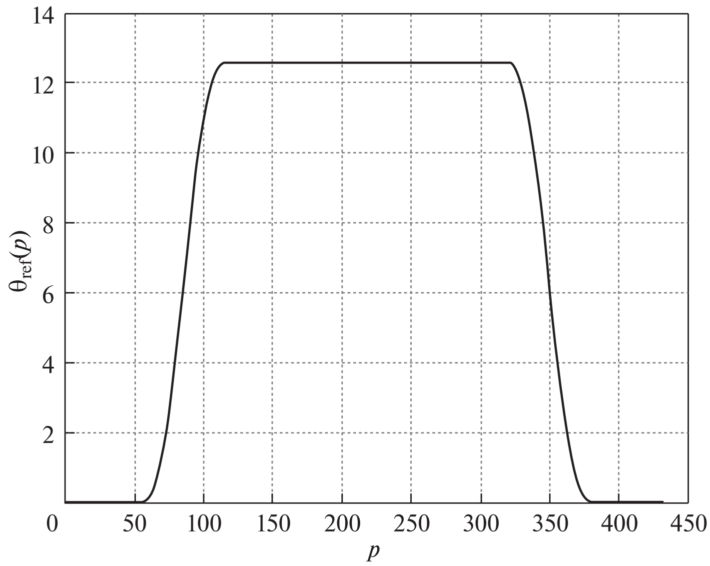

Fig. 2. The reference trajectory of the drive shaft angle.

learning error:

$$\mathrm{RMS}(e_k) = \sqrt{\frac{1}{N}\sum_{p=0}^{N-1} ||e_k(p)||^2}. \tag{5.4}$$

Figure 1 shows the pass-to-pass progression of this error under different saturation levels.

To indicate the values close to the steady-state ones, the number of passes was taken sufficiently large ($k = 600$). According to the simulation results, the steady-state error increases by approximately 100 times when changing the saturation level from 4.3 A to 4.0 A. Figure 2 presents the reference trajectory of the shaft angle. Next, Figs. 3 and 4 show the pass-to-pass progressions of

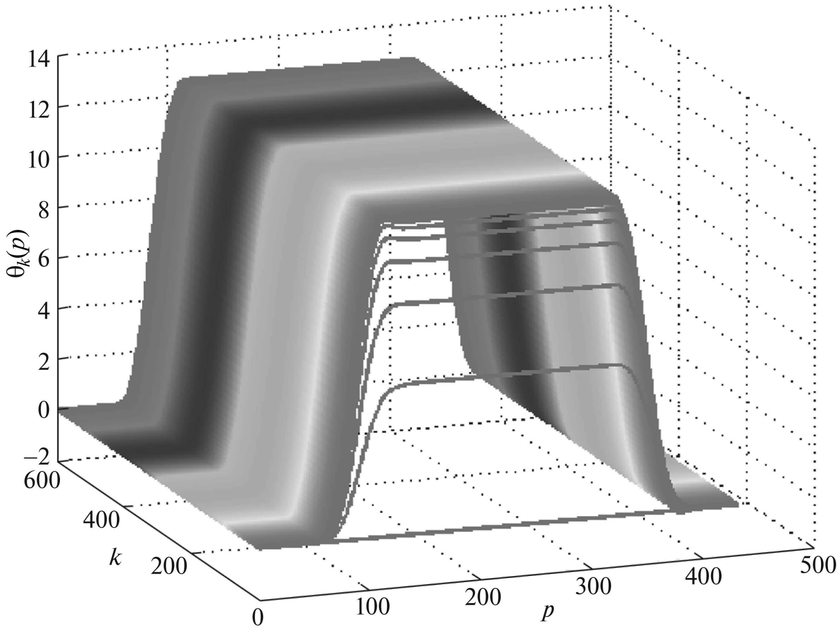

Fig. 3. The drive shaft angle progression under the saturation level $U = 4.3$.

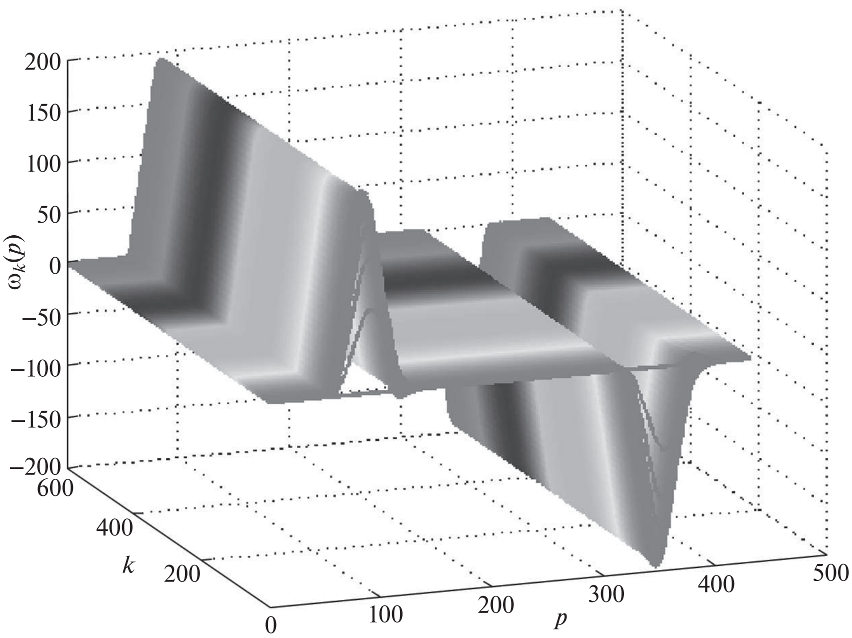

Fig. 4. The angular velocity progression under the saturation level $U = 4.3$.

the drive shaft angle and angular velocity, respectively. Finally, Figs. 5 and 6 demonstrate the pass-to-pass progressions of the control signal and learning error, respectively.

6. CONCLUSIONS

The ILC law designed in this paper corresponds to a definite delay and does not ensure convergence of the learning error under another delay. At the same time, it seems interesting to establish a similar result for a variable delay from a given range. As noted in the Introduction, ILC cor-

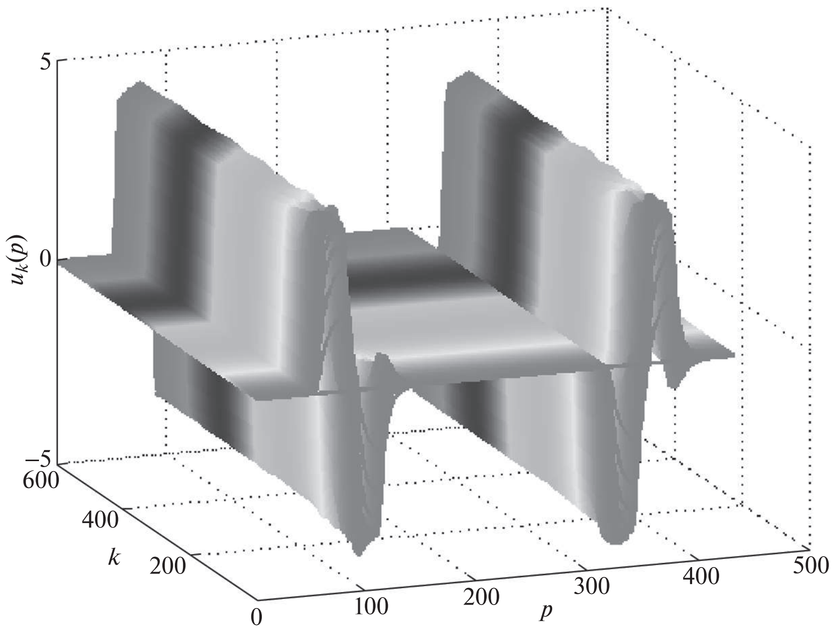

Fig. 5. The control signal progression under the saturation level $U = 4.3$.

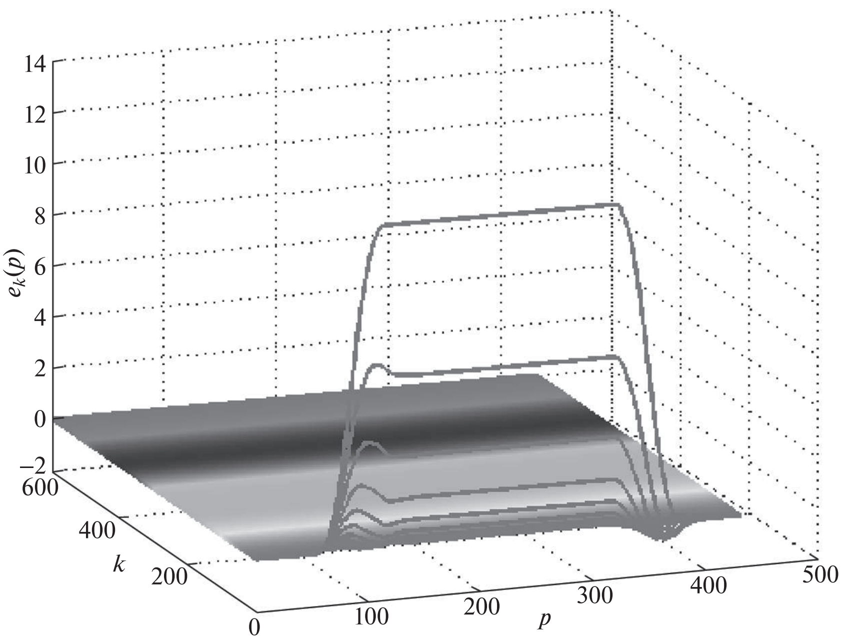

Fig. 6. The learning error progression under the saturation level $U = 4.3$.

rects the input signal without changing the system structure, and achieving the required accuracy depends on both the information structure and power of the input signal. In the case of input saturation, the signal power is limited, and the marginal error as $k \to \infty$ stabilizes near some nonzero value; hence, the required accuracy may not be achieved. On the other hand, without saturation, the trained control has a natural bound, and the best result will be achieved when this bound lies inside the saturation domain. Otherwise, it is necessary to carefully examine the saturation effect on accuracy degradation. As shown by the example above, this effect can be significant. In practice, such analysis will guide to selecting a drive of the right power.

The proposed approach has a definite drawback: there is no explicit dependence of the convergence rate of the learning error and achievable accuracy on the delay and saturation level.

Future research may aim at developing ILC algorithms under delay along the passes (remote control) and mixed delay (along the passes and with respect to the passes simultaneously).

FUNDING

This work was supported by the Russian Science Foundation, project no. 22-21-00612; https://rscf.ru/project/22-21-00612/

REFERENCES

1. Arimoto, S., Kawamura, S., and Miyazaki, F., Bettering Operation of Robots by Learning, *J. Robot. Syst.*, 1984, vol. 1, pp. 123–140.

2. Freeman, C.T., Rogers, E., Hughes, A.-M., Burridge, J.H., and Meadmore, K.L., Iterative Learning Control in Health Care: Electrical Stimulation and Robotic-Assisted Upper-Limb Stroke Rehabilitation, *IEEE Control Syst. Magaz.*, 2012, vol. 47, pp. 70–80.

3. Meadmore, K.L., Exell, T.A., Hallewell, E., Hughes, A.-M., Freeman, C.T., Kutlu, M., Benson, V., Rogers, E., and Burridge, J.H., The Application of Precisely Controlled Functional Electrical Stimulation to the Shoulder, Elbow and Wrist for Upper Limb Stroke Rehabilitation: A Feasibility Study, *J. of NeuroEngineer. and Rehabilitation*, 2014, pp. 11–105.

4. Ketelhut, M., Stemmler, S., Gesenhues, J., Hein, M., and Abel, D., Iterative Learning Control of Ventricular Assist Devices with Variable Cycle Durations, *Control Engineer. Practice*, 2019, vol. 83, pp. 33–44.

5. Sammons, P.M., Gegel, M.L., Bristow, D.A., and Landers, R.G., Repetitive Process Control of Additive Manufacturing with Application to Laser Metal Deposition, *IEEE Transact. Control Syst. Technol.*, 2019, vol. 27, no. 2, pp. 566–575.

6. Lim, I., Hoelzle, D.J., and Barton, K.L., A Multi-objective Iterative Learning Control Approach for Additive Manufacturing Applications, *Control Engineer. Practice*, 2017, vol. 64, pp. 74–87.

7. Sornmo, O., Bernhardsson, B., Kroling, O., Gunnarsson P., and Tenghamn, R., Frequency-Domain Iterative Learning Control of a Marine Vibrator, *Control Engineer. Practice*, 2016, vol. 47, pp. 70–80.

8. Hladowski, L., Galkowski, K., Cai, Z., Rogers E., Freeman, C., and Lewin, P., Experimentally Supported 2D Systems Based Iterative Learning Control Law Design for Error Convergence and Performance, *Control Engineer. Practice*, 2010, vol. 18, pp. 339–348.

9. Bristow, D.A., Tharayil, M., and Alleyne, A.G., A Survey of Iterative Learning Control: A Learning-Based Method for High-Performance Tracking Control, *IEEE Control Syst. Magaz.*, 2006, vol. 26, no. 3, pp. 96–114.

10. Ahn, H-S., Chen, Y.Q., and Moore, K.L., Iterative Learning Control: Survey and Categorization, *IEEE Trans. Syst. Man Cybern. Part C: Appl. Rev.*, 2007, vol. 37, no. 6, pp. 1099–1121.

11. Xu, J-X., Tan, Y., and Lee, T.-H., Iterative Learning Control Design Based on Composite Energy Function with Input Saturation, *Automatica*, 2004, vol. 40, pp. 1371–1377.

12. Mishra, S., Topcu, U., and Tomizuka, M., Iterative Learning Control with Saturation Constraints, *Proc. 2009 American Control Conf.*, 2009, pp. 943–948.

13. Zhang, R. and Chi, R., Iterative Learning Control for a Class of MIMO Nonlinear System with Input Saturation Constraint, *Proc. 36th Chinese Control Conf.*, 2017, pp. 3543–3547.

14. Lješnjanin, M., Tan, Y., Oetomo, D., and Freeman, C.T., Spatial Iterative Learning Control: Systems with Input Saturation, *2017 American Control Conf.*, 2017, pp. 5121–5126.

15. Wei, Z.-B., Quan, Q., and Cai, K.-Y., Output Feedback ILC for a Class of Nonminimum Phase Nonlinear Systems with Input Saturation: An Additive-State-Decomposition-Based Method, *IEEE Trans. Autom. Control*, 2017, vol. 62, pp. 502–508.

16. Sebastian, G., Tan, Y., Oetomo, D., and Mareels, I., Iterative Learning Control for Linear Time-varying Systems with Input and Output Constraints, *2018 Australian and New Zealand Control Conf. (ANZCC)*, 2018, pp. 87–92.

17. Sebastian, G., Tan, Y., and Oetomo, D., Convergence Analysis of Feedback-Based Iterative Learning Control with Input Saturation, *Automatica*, 2019, vol. 101, pp. 44–52.

18. Chen, Y., Gong, Z., and Wen, C., Analysis of a High-Order Iterative Learning Control Algorithm for Uncertain Nonlinear Systems with State Delays, *Automatica*, 1998, vol. 34, pp. 345–353.

19. Liu, T., Gao, F., and Wang, Y., IMC-based Iterative Learning Control for Batch Processes with Uncertain Time Delay, *Journal of Process Control*, 2010, vol. 20, pp. 173–180.

20. Wang, L., Mo, S., Zhou, D., Gao, F., and Chen, X., Delay-Range-Dependent Robust 2D Iterative Learning Control for Batch Processes with State Delay and Uncertainties, *Journal of Process Control*, 2013, vol. 23, pp. 715–730.

21. Tao, H., Paszke, W., Yang, H., and Gałkowski, K., Finite Frequency Range Robust Iterative Learning Control of Linear Discrete System with Multiple Time-Delays, *Journal of the Franklin Institute*, 2019, vol. 356, pp. 2690–2708.

22. Tao, H., Paszke, W., Rogers, E., Yang, H., and Gałkowski, K., Finite Frequency Range Iterative Learning Fault-Tolerant Control for Discrete Time-Delay Uncertain Systems with Actuator Faults, *ISA Transactions*, 2019, vol. 95, pp. 152–163.

23. Browne, F., Rees, B., Chiu, G.T.-C., and Jain, N., Iterative Learning Control with Time-Delay Compensation: An Application to Twin-Roll Strip Casting, *IEEE Trans. Control Systems Technology*, 2021, vol. 29, pp. 140–149.

24. Pakshin, P., Emelianova, J., Rogers, E., and Galkowski, K., Iterative Learning Control with Input Saturation, *IFAC PapersOnLine*, 2019, vol. 52, no. 29, pp. 338–343.

25. Rogers, E., Galkowski, K., and Owens, D.H., *Control Systems Theory and Applications for Linear Repetitive Processes*, Lect. Notes Control Inform. Sci., vol. 349, Berlin: Springer-Verlag, 2007.

26. Pakshin, P., Emelianova, J., Emelianov, M., Galkowski, K., and Rogers, E., Dissipivity and Stabilization of Nonlinear Repetitive Processes, *Syst. & Control Lett.*, 2016, vol. 91, pp. 14–20.

27. Emelianova, J.P. and Pakshin, P.V., Iterative Learning Control Design Based on State Observer, *Automation and Remote Control*, 2019, vol. 80, pp. 1561–1573.

28. Tarbouriech, S., Garcia, G., Gomes da Silva Jr., J.M., and Queinnec, I., *Stability and Stabilization of Linear Systems with Saturating Actuators*, London: Springer-Verlag, 2011.

29. Yakubovich, V.A., Leonov, G.A., and Gelig, A.Kh., *Stability of Stationary Sets in Control Systems with Discontinuous Nonlinearities*, London: World Scientific Press, 2004.

30. Mandra, S., Galkowski, K., and Aschemann, H., Robust Guaranteed Cost ILC with Dynamic Feedforward and Disturbance Compensation for Accurate PMSM Position Control, *Control Engineering Practice*, 2017, vol. 65, pp. 36–47.

This paper was recommended for publication by N.V. Kuznetsov, a member of the Editorial Board